Proc. Natl. Acad. Sci. USA
Vol. 75, No. 6, pp. 2764–2766, June 1978
Biophysics

Direct evidence for 6-fold symmetry of the herpesvirus hexon capsomere

(scanning transmission electron microscopy)

DEIRDRE FURLONG

The Enrico Fermi Institute, The University of Chicago, 5630 S. Ellis Avenue, Chicago, Illinois 60637

Communicated by Albert V. Crewe, April 10, 1978

ABSTRACT **Rotational power spectrum analysis of scanning transmission electron micrographs of negatively stained herpesvirus capsids has given direct evidence for the 6-fold symmetry of the herpesvirus hexon capsomere. Individual hexons have been analyzed *in situ* without interference from other parts of the capsid because only one level of the capsid was in focus in the micrograph. This study found hexons to have 6-fold symmetry. The majority of the mass of each hexon subunit was seen to lie on a line connecting the centers of adjacent capsomeres. This agrees with analysis of conventional micrographs of capsid fragments, which are also presented, as well as with biochemical data and theoretical expectations.**

One feature of the scanning transmission electron microscope (STEM) yet to be exploited is the differential focusing of the beam at different levels in the specimen (1). In the STEM the beam is conical. Wave optical calculations indicate that, for a beam convergence half-angle of 16 milliradians (2) and a 5-Å-diameter probe size at the carbon support film, the probe or beam size would be approximately 40 Å in diameter at 900 Å below the support film (Fig. 1). This indicated that an object 800–1000 Å thick below such a film would be in focus at the side next to the carbon film and out of focus on its other side. These considerations made it possible to get information about only one level of a complex object.

A suitable and interesting object for such a study would be the capsid of a large icosahedral virus. Herpesvirus type 1 nucleocapsids were chosen for this study. The nucleocapsid consists of a hollow protein shell, capsid, P = 1; T = 16 (3–5), 1000 Å in diameter around a DNA-containing core. Conventional electron microscopy of negatively stained capsids images both sides of the capsid simultaneously, superimposed on one another, because of the large depth of focus of that instrument. Elaborate reconstruction methods have been used to determine the structures of several small spherical viruses (6–10) but have so far been impractical for large viruses. However, the structure of capsid subunits (capsomeres) of large viruses has been observed directly in fragments of broken capsids (11–14).

As described above, the STEM offers the opportunity to obtain an in-focus image of one side of the capsid. The image contribution from the other side would be so defocused as to contribute no fine structure information. Capsids present a known symmetry that allows one to tell whether both sides contribute to the image. When looking down the 3- or 5-fold symmetry axis of the capsid, the upper and lower sides can be considered to be identical structures rotated with respect to each other by 180° and separated by approximately 800 Å. The hexons are expected to have 6-fold symmetry and to be related to one another by 3-fold symmetry. If both sides of the capsid contribute to the image, both the hexon and the intercapsomeric 3-fold site would have 6-fold or pseudo-6-fold symmetry. If only one side was contributing to the in-focus image, the hexon would have 6-fold symmetry and the center amid three adjacent capsomeres would be 3-fold.

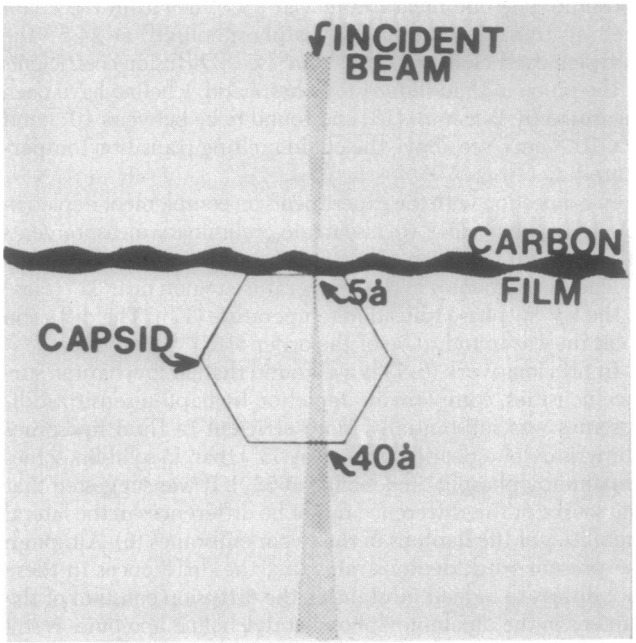

FIG. 1. Drawing (not to scale) illustrating how the conical beam can be focused to yield only one side of the object in sharp focus.

METHODS

To demonstrate these ideas experimentally, fresh herpes simplex virus type 1 nucleocapsids were prepared by the method of Gibson and Roizman (15). Five microliters of capsid suspension was put on a thin carbon (<50 Å) film supported on a 400-mesh copper grid. After 1 min, excess fluid was drawn off and 20 μl of 2% uranyl acetate in distilled water was added. The stain was drawn off and the grid was allowed to air dry. Fresh nucleocapsid preparations were used for whole capsids. For disrupted capsids and fragments, the capsid suspension was frozen and thawed two or three times. No protease was used, to avoid unnecessary damage to the capsomeres.

The fragments were examined in a Siemens 101 electron microscope operated at 80 kV with a 200-μm condenser aperture and a 300-μm objective aperture. The bright-field image was recorded on Kodak EM 4489 film. The grid was inserted specimen side up. No special effort was made to decrease the electron dose, but images were recorded immediately after focusing.

The costs of publication of this article were defrayed in part by the payment of page charges. This article must therefore be hereby marked "*advertisement*" in accordance with 18 U.S.C. §1734 solely to indicate this fact.

Abbreviation: STEM, scanning transmission electron microscope.

Whole capsids were examined in the STEM described by Wall *et al.* (2). The elastically scattered electrons were used to form the image. Because elastic scattering is approximately proportional to $Z^{3/2}$ (16), and uranyl acetate has an atomic number much greater than the average for DNA or protein, this scattering mainly reflected the stain distribution. After the grid was inserted specimen side down, the microscope was focused on the carbon support film at high magnification. Then the magnification was decreased and the image of the first or second scan of a field of capsids was recorded on Kodak 35 mm TRI-X film. This corresponds to a dose of 100 el/Å^2. For computer analysis, selected images were photographically enlarged on Kodak 7302 professional film and the optical density was measured on an Optronix drum scanner controlled on line by a PDP 11/40 computer. The enlargement was chosen such that the scan sampled the image at intervals corresponding to 4 Å in the object. The rotational power spectra were determined by using Fortran programs written by T. Wellems and S. Fuller (at The University of Chicago), similar to those developed by Crowther and Amos (17) and used by Crowther and Franklin (12) for adenovirus capsid fragments.

RESULTS

By conventional electron microscopy, capsids that had been frozen and thawed three times showed mostly unbroken capsids, but a few broken capsids and fragments of capsids were seen. The breaks often occurred along the edge between facets, through capsomeres. In the fragments, capsomeres could be recognized but most capsomeres had peripheral material attached to them. The capsomeres present in one analyzed fragment had a center-to-center spacing of 130 Å, larger than the approximately 120-Å spacing seen in the capsomeres in the capsids. Conventional transmission electron micrographs of a typical capsid and of a fragment used for power spectrum are shown in Fig. 2 *a* and *b*, respectively. The fragment has four recognizable capsomeres. There is also some material present at the periphery of the group, as if parts of adjacent capsomeres or intercapsomeric structures had remained attached. The region analyzed when the power spectrum of a capsomere was calculated included this material. A square box was used to mask off all particles or groups of particles.

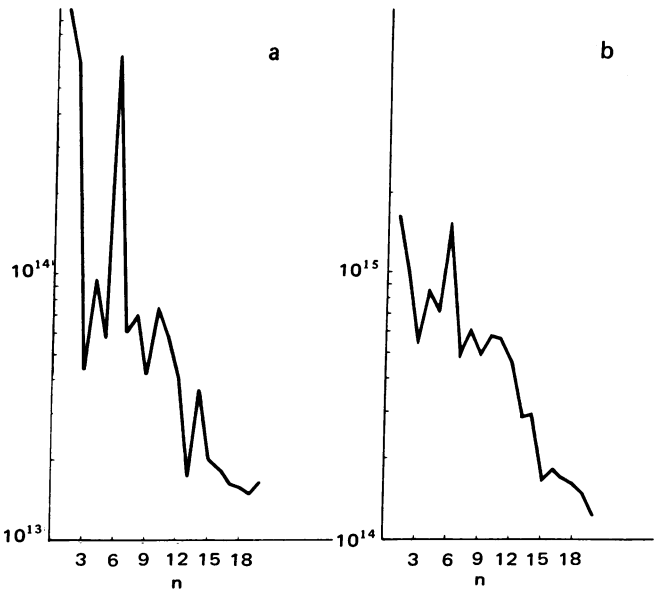

FIG. 3. Rotational power spectra of the capsomeres indicated by the arrows in Fig. 2. (*a*) Spectrum from the conventional transmission electron image of the capsid fragment. (*b*) Spectrum of the STEM image of the whole capsid.

The power spectrum from one of the capsomeres (arrows in Fig. 2) is presented in Fig. 3*a*. The 6-fold peak is strong and the 3-fold peak is depressed. The higher-order harmonics are not strong for any symmetry. In three of the four capsomeres seen in Fig. 2*b*, the 6-fold peak dominated and the 3-fold was depressed. In the fourth (furthest right) capsomere, which was visibly distorted, no clear symmetry was seen.

A STEM micrograph of negatively stained whole capsids is shown in Fig. 2*c*. The particles appear to be lying on a facet with the 3-fold capsid axis parallel to the beam path. The center-to-center distance for the three central capsomeres in the

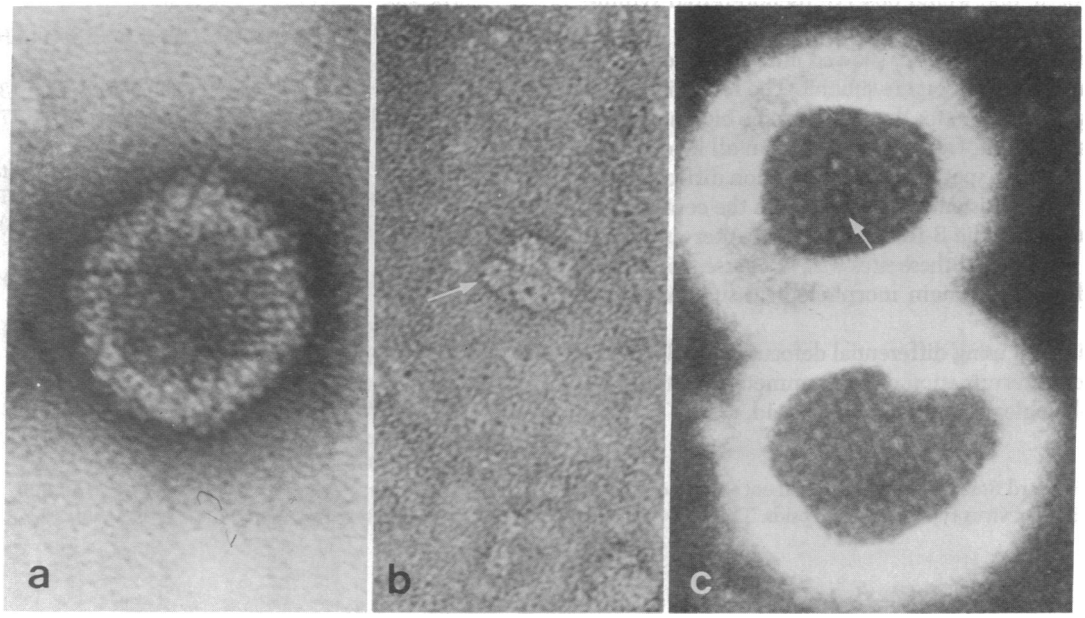

FIG. 2. Electron micrographs of negatively stained herpesvirus type 1 nucleocapsids and capsid fragment. (*a* and *b*) Conventional transmission electron micrographs of a capsid and a capsid fragment containing four capsomeres. Protein is white (×400,000.) (*c*) STEM micrograph of two capsids. Stain is white. (×500,000.)

facet (using the 6-fold symmetry center) was 122 Å in all three cases. Because the particle was heavily stained, the beam was completely scattered by the stain, so no detail of the facet corners can be seen.

The power spectrum of the three central and six of the edge capsomeres was calculated. The area chosen for each analysis extended to the region surrounding the capsomere in question but not to the adjacent capsomeres, so that material from the six neighboring capsomeres did not contribute to the spectrum. The power spectrum of one capsomere (arrow) in the capsid in Fig. 2*c* is presented in Fig. 3*b*. The 6-fold peak is seen to dominate but harmonics 12 and above are not strong. In each analysis of capsomeric symmetry in the intact capsid, the spectrum was noisy and the higher harmonics (above 12) were not above the variation due to noise. In each case, the 6-fold peak was very strong and the 3-fold peak was depressed for each of the central capsomeres. The staining of the edge capsomeres was less even and the spectra were more noisy. In each capsid examined, only the three central capsomeres showed strong 6-fold symmetry. No capsomere with five nearest neighbors, penton, was examined. The outer capsomeres, those lying across a facet edge, showed less strong 6-fold symmetry or showed no clear symmetry. The power spectra of the capsomeres from the capsid fragment and in the capsid indicated 6-fold symmetry for the capsomere (Fig. 3).

The symmetry relationships among capsomeres were also determined to be sure that only one side was contributing to the image. The spectra at the center of three adjacent capsomeres in the fragment and in the capsid shown in Fig. 2 *b* and *c* are shown in Fig. 4 *a* and *b*, respectively. The capsomere arrangement shows strong 3-fold symmetry which is expected if the subunits were placed in a folded P-6 net. This icosadeltahedral arrangement of structural subunits is in good agreement with the biochemical evidence of 950–1000 copies of the major capsid protein per capsid (18). The 3-fold peak for the capsomere group was strong for the capsomeres in the capsid as well as in the fragment. If both sides of the capsid were focused to the same extent and the 3-fold axis of the capsid were parallel to the beam path, one would observe pseudo-6-fold symmetry.

The filtered images of capsids showed little agreement in the detailed outline of the capsomere subunit. The resolution of the STEM micrograph was better than 8 Å; but the high noise level over the capsid, arising from scattering from all levels of the object, made the high spatial frequency region difficult to interpret. Stain was consistently excluded from the center of the capsomere and from the 3-fold symmetry center amid capsomeres. The exclusion at these sites was, of course, not as great as at the radius of the main morphological subunits of the capsomeres.

This technique of using differential defocus in the STEM has allowed direct determination of the symmetries of the herpesvirus morphological subunits in the capsid.

I thank Dr. Bernard Roizman for encouragement and for exquisitely clean herpes simplex virus type 1 nucleocapsids. This study was supported by the U.S. Energy Research and Development Administration (EY-76-S-02-2398) and National Institutes of Health Biotechnology Resource Grant 5 P41 RR 00984.

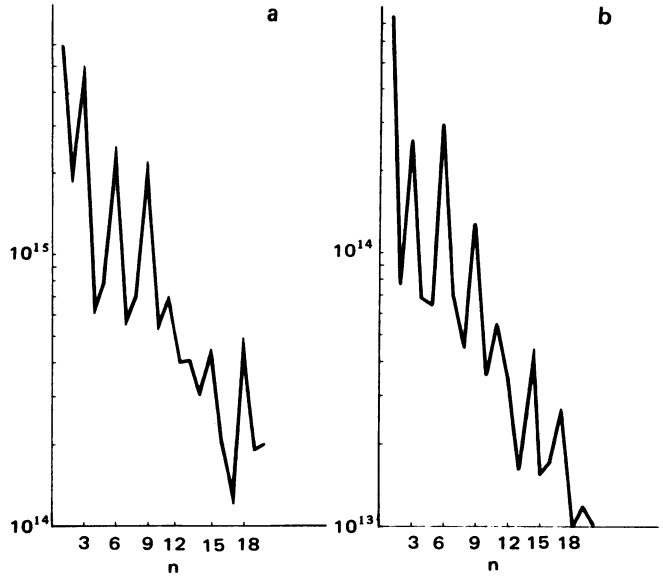

FIG. 4. Rotational power spectrum of the intercapsomeric region amid three capsomeres. (*a*) Spectrum from the three capsomeres to the left in Fig. 2*b*. (*b*) Spectrum from amid the three central capsomeres in the capsid on the right in Fig. 2*c*.

1. Crewe, A. V. & Wall, J. (1970) *J. Mol. Biol.* **48**, 375–393.
2. Wall, J., Langmore, J., Isaacson, M. S. & Crewe, A. V. (1974) *Proc. Natl. Acad. Sci.* **71**, 1–5.
3. Caspar, D. L. D. & Klug, A. (1962) Cold Spring Harbor Symp. *27*: 1–24.
4. Wildy, P., Russell, W. C., & Horne, R. W. (1960) *Virology* **12**, 204–222.
5. Wildy, P. & Watson, D. H. (1962) *Cold Spring Harbor Symp.* **27**, 25–47.
6. Crowther, R. A. (1971) *Phil. Trans Roy Soc. (London)*, A **317**, 319–360.
7. Crowther, R. A. & Amos, L. (1971) *Cold Spring Harbor Symp.* **36**, 489–494.
8. De Rosier, D. J. & Klug, A. (1968) *Nature* **217**, 130–134.
9. Winkler, F. K., Schutt, C. E., & Harrison, S. C. (1977) *Nature* **265**, 509–513.
10. Johnson, J. E., Argos, P. & Rossman, M. J. (1975) *Acta Crystallogr. Sec. B Struct. Crystallogr. Cryst. Chem.* **31**, 2577–2583.
11. Palmer, E. L., Martin, M. L. & Gary, G. W. (1975) *Virology* **65**, 260–265.
12. Crowther, R. A. & Franklin, R. M. (1972) *J. Mol. Biol.* **68**, 181–184.
13. Palmer, E. L. & Martin, M. (1977) *Virology* **76**, 109–113.
14. Vernon, S. K., Lawrence, W. C. & Cohen, G. H. (1974) *Intervirology* **4**, 237–248.
15. Gibson, W. & Roizman, B. (1972) J. Virol **10**, 1044–1052.
16. Langmore, J. P., Wall, J. & Isaacson, M. S. (1973) *Optik Stuttgart* **38**, 335–350.
17. Crowther, R. A. & Amos, L. (1971) *J. Mol. Biol.* **60**, 123–130.
18. Honess, R. & Roizman, B. (1973) *J. Virol.* **12**, 1347–1365.